The Astrophysical Journal, 676: L93–L96, 2008 April 1

COSMIC MICROWAVE BACKGROUND–WEAK LENSING CORRELATION: ANALYTICAL AND NUMERICAL STUDY OF NONLINEARITY AND IMPLICATIONS FOR DARK ENERGY

Atsushi J. Nishizawa,[1] Eiichiro Komatsu,[2] Naoki Yoshida,[1] Ryuichi Takahashi,[1] and Naoshi Sugiyama[1,3]
Received 2007 November 12; accepted 2008 February 21; published 2008 March 3

ABSTRACT

Evolution of density fluctuations yields secondary anisotropies in the cosmic microwave background (CMB), which are correlated with the same density fluctuations that can be measured by weak lensing (WL) surveys. We study the CMB-WL correlation induced by the integrated Sachs-Wolfe (ISW) effect and its nonlinear extension, the Rees-Sciama (RS) effect, using analytical models as well as *N*-body simulations. We show that an analytical model based on the time derivative of matter power spectrum agrees with simulations. All-sky cosmic-variance-limited CMB and WL surveys allow us to measure the correlation from the nonlinear RS effect with high significance (50 σ) for $l_{\rm max} = 10^4$, whereas forthcoming missions such as *Planck* and LSST are expected to yield 1.5 σ detections, on the assumption of that the point-source contributions are negligible. We find that the CMB-WL correlation has a characteristic scale which is sensitive to the nature of dark energy.

Subject headings: cosmic microwave background — cosmology: theory — large-scale structure of universe

1. INTRODUCTION

Secondary temperature anisotropies of the cosmic microwave background (CMB) provide invaluable information on the structure formation in the universe. The sources of anisotropies include the Sunyaev-Zel'dovich (SZ) effects by galaxy clusters as well as by reionization, the integrated Sachs-Wolfe (ISW) effect, the Rees-Sciama (RS) effect, and CMB lensing. We shall use the term "ISW" when the underlying matter fluctuation is linear, and "RS" when it is nonlinear.

The forthcoming *Planck* satellite[4] and ground-based observations such as the Atacama Cosmology Telescope (ACT; Kosowsky 2003) and South Pole Telescope (SPT; Ruhl et al. 2004) are designed to measure temperature fluctuations at arcminute scales, and thus are expected to detect some of the secondary anisotropies.

The RS effect is, in principle, a unique probe of the time variation of gravitational potential, as given by (Sachs & Wolfe 1967; Rees & Sciama 1968)

$$\frac{\Delta T(\hat{\boldsymbol{n}})}{T} = -2\int_0^{r_*} dr\Phi'(\hat{\boldsymbol{n}}r,\, r), \tag{1}$$

where Φ is the Newtonian potential, $\hat{\boldsymbol{n}}$ is a unit direction vector, r is the conformal look-back time, and r_* is r out to the photon-decoupling epoch. The prime denotes $\partial/\partial r$, which is equal to $-\partial/\partial\eta$, where η is the conformal time.

In the linear regime, Φ' vanishes in a matter-dominated universe; however, when either curvature or dark energy dominates, Φ decays in time and thus $|\Phi|' > 0$. In the nonlinear regime, on the other hand, Φ *grows* in time, $|\Phi|' < 0$. Therefore, one expects $\Phi\Phi' > 0$ on large scales where density fluctuations are still linear, and $\Phi\Phi' < 0$ on small scales where fluctuations are nonlinear.

The autocorrelation of this effect, both linear and nonlinear, has been studied (Seljak 1996; Tuluie et al. 1996; Cooray 2002a). The cross-correlation between the *linear* ISW effect and large-scale structure traced by galaxies has also been studied (e.g., Crittenden & Turok 1996; Peiris & Spergel 2000; Cooray 2002b; Afshordi 2004), and detected for various galaxy surveys (e.g., Boughn & Crittenden 2004; Nolta et al. 2004; Afshordi et al. 2004).

Much less attention has been given to the correlation of the *nonlinear* RS effect and large-scale structure. As this effect changes sign at the linear to nonlinear transition scale, the signature of nonlinearity is distinct.

The RS effect is not the only thing that is correlated with the large-scale structure. The SZ effects, as well as radio and infrared point sources, also trace the large-scale structure (Takada & Sugiyama 2002; Doré et al. 2004; Hirata et al. 2004). Fortunately, multifrequency data enable us to separate those contributions that have unique and specific frequency dependence (Hu et al. 1994; Tegmark & Efstathiou 1996). To this end, we need follow-up observations with high sensitivity and angular resolution, such as with the Atacama Large Millimeter Array (ALMA).[5]

In this Letter, we calculate the cross-correlation of the RS effect and large-scale structure traced by weak lensing (WL) surveys. In particular, we simulate this directly using an *N*-body code for the first time. We adopt the flat ΛCDM model with $(\Omega_{\Lambda 0}, \sigma_8, h, n_s) = (0.74, 0.76, 0.7, 1)$, which is consistent with Spergel et al. (2007).

2. ANALYTICAL MODEL

The amplitude of distortion in galaxy images due to WL is given by the so-called convergence, κ, which is proportional to the projected density field along the line of sight. As the Newtonian potential, Φ, is negatively proportional to density field via the Poisson equation, the sign of CMB-WL correlation is given by $\Phi\Phi'$ and, thus, positive on large scales and negative on small scales.

[1] Department of Physics, Nagoya University, Furocho, Nagoya, Aichi 464-8602, Japan; atsushi@a.phys.nagoya-u.ac.jp.
[2] Department of Astronomy, University of Texas, Austin, TX 78712.
[3] Institute for Physics and Mathematics of the Universe, University of Tokyo, 5-1-5 Kashiwa-no-Ha, Kashiwa City, Chiba 277-8582, Japan.
[4] See http://www.rssd.esa.int/index.php?project=Planck.
[5] See http://www.nro.nao.ac.jp/alma/E/index.html.

The cross-correlation of the RS effect and κ, C_l, is

$$C_l = 2l^2 \int_0^{r_*} dr\, P_{\Phi\Phi'}\left(\frac{l}{r},\, r\right) \int_z^{z_*} dz_s\, p(z_s)\, \frac{r_s - r}{r_s r^3}, \qquad (2)$$

where $P_{\Phi\Phi'}(k,\, r)$ is the power spectrum of $\Phi\Phi'$ at r, z_s is the redshift of source galaxies, and $r_s \equiv r(z_s)$. Here $p(z)dz$ is the probability of finding galaxies between z and $z + dz$. We use $p(z) = Az^2 \exp\,[-(z/z_0)^\beta]$, where A is a normalization factor determined by $\int_0^\infty p(z)dz = 1$ (Efstathiou et al. 1991). We consider two survey designs: model 1, a deep survey, $(\beta,\, z_0) = (0.7,\, 0.5)$, whose $p(z)$ peaks at $z \sim 2.2$ with a broad distribution; and model 2, a shallow survey, $(\beta,\, z_0) = (2,\, 0.9)$, which peaks at $z \simeq 0.9$ with a narrower distribution. We calculate $P_{\Phi\Phi'}$ from

$$P_{\Phi\Phi'}(k,\, r) = \frac{9\Omega_{m0}^2 H_0^4}{4a^2k^4}\, [P_{\delta\delta'}(k,\, r) - \mathcal{H}P_{\delta\delta}(k,\, r)], \qquad (3)$$

where $\mathcal{H} = -d \ln a/dr$, and $P_{\delta\delta}$ and $P_{\delta\delta'}$ are the power spectrum of density fluctuations, δ, and the cross-correlation of δ and δ', respectively.

How do we calculate $P_{\delta\delta'}$? It might be tempting to use $P_{\delta\delta'} = P'_{\delta\delta}/2$, as the following might seem obvious: $\langle\delta(\boldsymbol{k},\, r)\delta'(\boldsymbol{p},\, r)\rangle = (1/2)(\partial/\partial r)\langle\delta(\boldsymbol{k},\, r)\delta(\boldsymbol{p},\, r)\rangle$. However, this relation is exact only in the linear regime, for which the ensemble average (taken over initial perturbations) and $\partial/\partial r$ commute. As they do not generally commute in the nonlinear regime, we need to check whether this *Ansatz* is a good approximation in the nonlinear regime.

Before pursuing the fully nonlinear regime, we consider the *Ansatz* using third-order perturbation theory (3PT). We employ the expansion of $\delta(\boldsymbol{k},\, r)$ in a series up to the third order in the initial linear perturbation, $\delta_1(\boldsymbol{k})$, as $\delta(\boldsymbol{k},\, r) = \sum_{n=1}^{3} D^n(r)\delta_n(\boldsymbol{k})$. Here D is the linear growth factor and δ_n are of order δ_1^n. This simple factorization of time-dependent and scale-dependent terms is exactly correct in an Einstein–de Sitter universe. It is also known that this form of expansion gives a quite relevant estimation of the power spectrum for the ΛCDM model if the time-dependent term is simply replaced with the corresponding growth factor (Bernardeau et al. 2002; Jeong & Komatsu 2006). The above expansion warrants that the ensemble average and the time derivative commute. It is also true when the expansion above is truncated at a finite order instead of third order. Thus we can compute $P_{\Phi\Phi'}$ from equation (3) using 3PT and $P_{\delta\delta'} = P'_{\delta\delta}/2$.

Note that perturbation theory generally breaks down for $\delta \gtrsim 1$. We calculate C_l using 3PT to probe quasi-linear scales. Compared with C_l using N-body simulations, which we discuss in detail in the next section, 3PT predicts that the sign of C_l changes at smaller l because 3PT overestimates nonlinearity in $P_{\delta\delta}$ (Bernardeau et al. 2002; Jeong & Komatsu 2006). This indicates the limitations of PT.

3. ANALYTICAL MODEL VERSUS N-BODY SIMULATION

To test $P_{\delta\delta'} \approx P'_{\delta\delta}/2$ in the nonlinear regime, we compare the analytical model with N-body simulations. We employ 512^3 dark matter particles in a volume of $L_{\rm box} = 250\ h^{-1}$ Mpc and $40\ h^{-1}$ Mpc on a side. The simulations are performed by the GADGET-2 code (Springel 2005). The initial conditions are generated by a standard method using the Zel'dovich approximation. We dump outputs from $z = 0.01$ to 10 uniformly sampled in $\log\,(1 + z)$. For each output redshift, we dump adjacent two outputs in order to calculate δ' and Φ'.

In the top panel of Figure 1, we show the analytical model

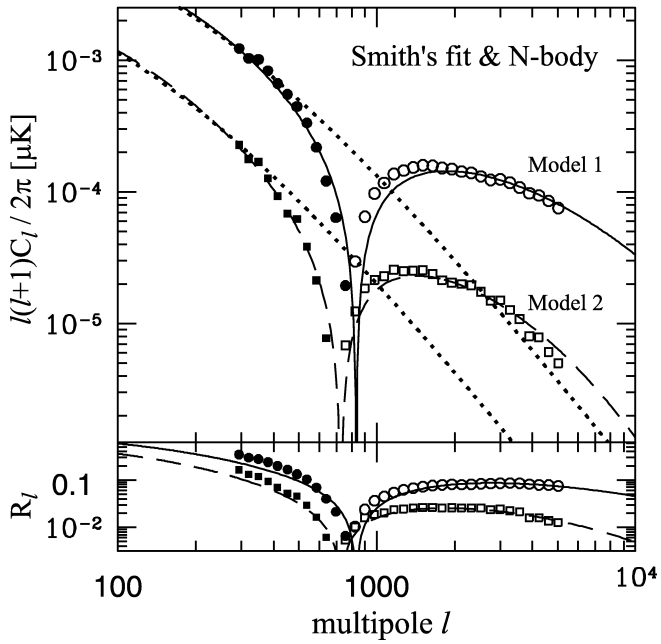

FIG. 1.—CMB-WL cross-correlation spectra, C_l, for two WL survey designs: deep (model 1) and shallow (model 2). *Top*: The symbols show C_l from the N-body simulation. The open and filled symbols show $C_l < 0$ and $C_l > 0$, respectively. The solid and long-dashed lines show the fully nonlinear model for models 1 and 2, respectively, while the dotted lines show the linear theory predictions. Note that the linear theory predicts $C_l > 0$ at all l. *Bottom*: CMB-WL cross-correlation coefficients, R_l.

of C_l with $P'_{\delta\delta}$ (solid and long-dashed lines show models 1 and 2, respectively), where $P_{\delta\delta}$ is the fully evolved nonlinear power spectrum (Smith et al. 2003), and the N-body results (open and filled symbols show negative and positive values, respectively). The agreement is good: the model describes the amplitude, shape, and crossover at $l \sim 800$ of C_l that are measured in the simulation. We therefore conclude that the *Ansatz*, $P_{\delta\delta'} \approx P'_{\delta\delta}/2$, is indeed accurate, up to $l = 5000$, where we can trust resolution of our N-body simulation. The cross-power calculated by 3PT generally agrees well with these results in the linear and quasi-linear regimes. We mention that, compared with the simulation result, 3PT overestimates $P_{\delta\delta}$ as explained above. The applicability of 3PT for computing C_l may be limited to linear and quasi-linear scales.

How well are RS (or ISW) and WL correlated? In the bottom left panel of Figure 1, we show the 2D correlation coefficient, $R_l = C_l/(C_l^\kappa C_l^{\rm RS})^{1/2}$. We have used the same nonlinear $P_{\delta\delta}$ to calculate the power spectrum of convergence, C_l^κ, while we have used the halo model approach (Cooray & Sheth 2002) to calculate that of RS, $C_l^{\rm RS}$. In the linear regime, ISW and κ are strongly correlated, $R_l \simeq 1$ (it is not exactly 1 because of the projection effect). The correlation weakens as nonlinearity becomes important: $R_l \simeq -0.05$ to -0.1 at $1000 \lesssim l \lesssim 10^4$ for model 1, and $R_l \simeq -0.01$ to -0.03 for model 2.

The weak correlation of C_l is due to the fact that Φ and Φ' are not correlated very well in the nonlinear regime: the 3D correlation coefficient, $R_{\rm 3D}(k) = P_{\Phi\Phi'}(k)/[P_\Phi(k)P_{\Phi'}(k)]^{1/2}$, reaches the maximal value, $R_{\rm 3D}(0.5/{\rm Mpc}) \simeq 0.2$, at $z = 1$, where the RS effect becomes largest. The 2D correlation, R_l, is even weaker than $R_{\rm 3D}(k)$ because of the projection effect and a mismatch between the redshift at which WL becomes largest ($z \simeq 0.5$) and that for the RS effect ($z \simeq 1$). The weak correlation makes it challenging to measure the CMB-WL correlation from nonlinearity.

To see where the cross-correlation signals come from, we

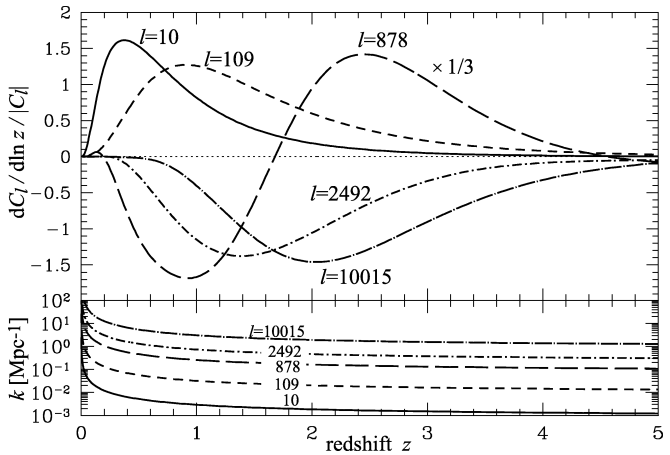

FIG. 2.—*Top*: Contribution to C_l from each redshift per logarithmic redshift interval, normalized by the absolute value of C_l, $(dC_l/d\ln z)/|C_l|$. The amplitude of the long-dashed line is 1/3 of the actual one. *Bottom*: Relation between k and l, $k = l/r(z)$, as a function of redshift.

show $dC_l/d\log z/|C_l|$ in Figure 2. On large angular scales, $l \sim 10$–100, the physical scale is larger than 1 Mpc, the correlations come from $z \lesssim 2$, and the sign is positive; thus, they are the linear ISW effect. On small angular scales, $l \sim 2500$–10^4, the physical scale is smaller than 1 Mpc, and the sign is negative; thus, they are the totally nonlinear RS effect. On the intermediate scale, $l = 800$, negative correlations come from lower redshifts, whereas positive ones come from higher redshifts. These correlations nearly cancel after the line-of-sight integration.

4. DETECTING NONLINEAR REES-SCIAMA EFFECT

Can we detect nonlinearity, $C_l < 0$? The signal-to-noise ratio (S/N) of C_l is given by

$$\left(\frac{\mathrm{S}}{\mathrm{N}}\right)^2_{l_{\max}} = f_{\mathrm{sky}} \sum_{l=2}^{l_{\max}} \frac{2l+1}{1+\left(\tilde{C}_l^{\mathrm{CMB}}\tilde{C}_l^{\kappa}/C_l^2\right)}, \tag{4}$$

where f_{sky} is the fraction of sky observed, and $\tilde{C}_l^{\mathrm{CMB}}$ and $\tilde{C}_l^{\kappa}$ are the total (signal plus noise) power spectra of the CMB (including primary, CMB lensing and the RS effect) and WL, respectively. The noise spectra of the CMB and WL surveys are given, respectively, by (Knox 1995; Schneider 2005)

$$N_l^{\mathrm{CMB}} = \sigma_{\mathrm{pix}}^2\theta_{\mathrm{fwhm}}^2 \exp\left[l(l+1)\theta_{\mathrm{fwhm}}^2/8\ln 2\right], \tag{5}$$

$$N_l^{\kappa} = \sigma_{\gamma}^2/n_{\mathrm{gal}}, \tag{6}$$

where σ_{pix} is the temperature noise per pixel, θ_{fwhm} is the FWHM of a Gaussian beam, n_{gal} is the number density of galaxies observed in a WL survey, and σ_{γ} is the noise in shear measurements, including intrinsic ellipticities.

We forecast S/N for the forthcoming surveys with the following parameters: $(f_{\mathrm{sky}}, \sigma_{\gamma}, n_g/\mathrm{arcmin}^2) = (0.024, 0.3, 20)$ for the Canada-France-Hawaii Telescope Legacy Survey (CFHTLS), (0.8, 0.1, 100) for the Large Synoptic Survey Telescope (LSST), $(f_{\mathrm{sky}}, \sigma_{\mathrm{pix}}, \theta_{\mathrm{FWHM}}) = (0.024, 2, 1.7')$ for ACT, and (0.8, 2.5/2.2/4.8, 9.5′/7.1′/5′) for *Planck* with 3 lowest frequency HFI channels. In Figure 3 we show the predicted S/N as a function of the maximum multipole $l_{\max}$ for cosmic-variance-limited CMB and WL (deep and shallow) surveys, as well as for the forthcoming surveys: *Planck* correlated with LSST, and ACT correlated with CFHTLS.

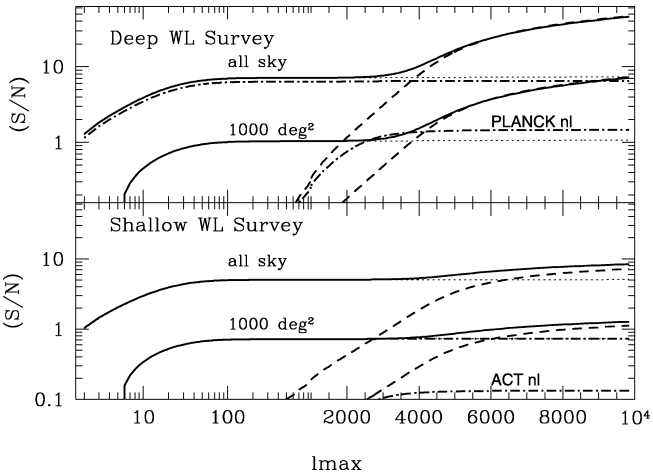

FIG. 3.—S/N as a function of the maximum multipole, $l_{\max}$. The dotted and dashed lines show the linear ISW and nonlinear RS effects, respectively, while the solid lines show the total, for cosmic-variance-limited CMB and WL surveys with all-sky (*upper curves*) and 1000 deg^2 sky coverage (*lower curves*). *Top*: Deep WL survey. The dash-dotted lines show S/N expected from *Planck*'s CMB data correlated with LSST's WL data. "PLANCK nl" shows the nonlinear RS only. *Bottom*: Shallow WL survey. Same as the top panel, but for ACT's CMB data correlated with CFHTLS's WL data.

We find that S/N is totally dominated by the linear ISW effect (*dotted lines*) at $l \lesssim 3000$, and then becomes dominated by the nonlinear RS effect (*dashed lines*) at higher l. All-sky CMB and WL surveys can yield S/N ~ 50 (10) for deep (shallow) WL surveys, whereas 1000 deg^2 surveys can only yield S/N ~ 7 (1). Once noise of the forthcoming surveys is included, however, S/N from the nonlinear RS effect becomes small compared to the linear ISW effect. For *Planck*+LSST we find S/N ~ 1.5 for the nonlinear RS effect, and 6 for the linear ISW effect. For ACT+CFHTLS we find S/N ~ 0.1 for nonlinear RS and 0.7 for linear ISW. Therefore, we conclude that these forthcoming surveys are not expected to yield significant detection of the nonlinear RS effect.

5. SENSITIVITY TO DARK ENERGY PARAMETERS

As the linear ISW effect vanishes during the matter era, it is sensitive to dark energy (DE) (e.g., Boughn & Crittenden 2004; Nolta et al. 2004; Afshordi et al. 2004). The nonlinear RS effect measures the structure growth, which is also sensitive to DE (Verde & Spergel 2002; Giovi et al. 2005). The crossover at $l \sim 800$, at which the linear and nonlinear contributions cancel, is particularly a unique probe of DE. Figure 4 shows the sensitivity of C_l to DE parameters: $\partial C_l/\partial\Omega_{\Lambda 0}$, $\partial C_l/\partial w_0$, and $\partial C_l/\partial w_1$. We use a simple form of the DE equation of state, $w(a) = p_{\Lambda}(a)/\rho_{\Lambda}(a)$, given by $w(a) = w_0 + w_1(1-a)$. The fiducial values are $w_0 = -1$ and $w_1 = 0$. We find $\partial C_l/\partial w_0 > 0$ and $\partial C_l/\partial w_1 > 0$ at all l. By increasing w_0 or w_1, one makes $w(a)$ less negative which, in turn, makes DE more important at earlier times. This does two things. On large scales where $C_l > 0$, it enhances the linear ISW effect, making C_l even more positive. On small scales where $C_l < 0$, it reduces the growth of nonlinear structure, making C_l less negative. In both cases we find positive derivatives. Dependence on $\Omega_{\Lambda 0}$ is slightly more complex. While $\partial C_l/\partial\Omega_{\Lambda 0} > 0$ at most l can be explained by the same physics as above, we find $\partial C_l/\partial\Omega_{\Lambda 0} < 0$ in the intermediate l. This is due to the assumption of a flat universe: a larger $\Omega_{\Lambda 0}$ results in a smaller Ω_{m0}, which alters the shape of $P_{\delta\delta}(k)$ with the peak shifted to larger scales. (A smaller Ω_{m0} delays matter-radiation equality.) Note that these dependencies

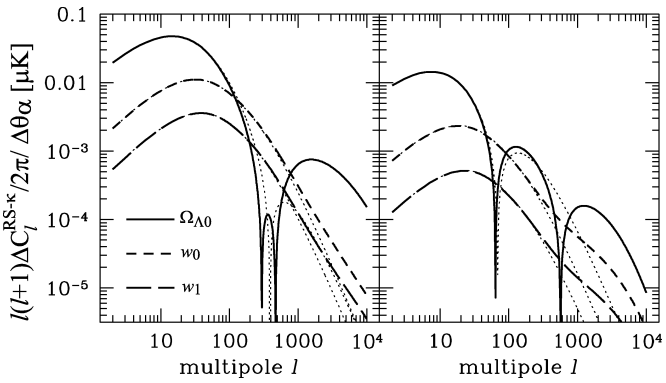

FIG. 4.—Sensitivity of the CMB-WL correlation to DE. Derivatives of C_l with respect to the DE parameters. The solid, short-dashed, and long-dashed curves show $\partial C_l/\partial\Omega_{\Lambda 0}$, $\partial C_l/\partial w_0$, and $\partial C_l/\partial w_1$, respectively. The thin dotted lines show curves from linear theory.

might be affected by DE clustering and the galaxy distribution of WL as well.

6. CONCLUSION

We have studied the cross-correlation between the CMB (the linear ISW effect as well as the nonlinear RS effect) and large-scale structure traced by WL. We have developed a simple analytical model based on the time derivative of the nonlinear matter power spectrum, and tested its validity analytically with third-order PT as well as numerically with *N*-body simulations.

We have shown that all-sky cosmic-variance-limited CMB and deep (shallow) WL surveys can yield a 50 σ (10 σ) detection of the *nonlinear* CMB-WL correlation for $l_{\rm max} = 10^4$. The forthcoming surveys are not expected to yield significant detections. We expect ~1.5 σ from *Planck*+LSST and 0.1 σ from ACT+CFHTLS.

Note that we have ignored the point-source contamination, which could be potentially important at very high multipoles, because point sources also trace the underlying large-scale density field. We may therefore need some follow-up observations with high sensitivities and angular resolutions, such as could be obtained using ALMA, in order to see how important the point-source contribution would be. The frequency range of ALMA is ~50 to 10^3 GHz and angular resolution can reach to 0.1″, which appears suitable for this purpose.

We claim that the change of the sign of C_l at the crossover, $l \sim 800$, offers a unique probe of the nature of DE. It might also be important in considering the effect of DE clustering and the source distribution of WL.

We thank Olivier Doré, Joe Hennawi, Ravi Sheth, and David Spergel for useful discussions and comments on the Letter. The work is supported by Grant-in-Aid for Scientific Research on Priority Areas No. 467 “Probing the Dark Energy through an Extremely Wide & Deep Survey with Subaru Telescope” and by the Mitsubishi Foundation. The numerical computations were done using cluster computers at Nagoya University. E. K. acknowledges support from an Alfred P. Sloan Fellowship.

REFERENCES

Afshordi, N. 2004, Phys. Rev. D, 70, 083536
Afshordi, N., Loh, Y., & Strauss, M. 2004, Phys. Rev. D, 69, 083524
Bernardeau, F., Colombi, S., Gaztanaga, E., & Scoccimarro, R. 2002, Phys. Rep., 367, 1
Boughn, S., & Crittenden, R. 2004, Nature, 427, 45
Cooray, A. 2002a, Phys. Rev. D, 65, 083518
———. 2002b, Phys. Rev. D, 65, 103510
Cooray, A., & Sheth, R. K. 2002, Phys. Rep., 372, 1
Crittenden, R. G., & Turok, N. 1996, Phys. Rev. Lett., 76, 575
Doré, O., Hennawi, J. F., & Spergel, D. N. 2004, ApJ, 606, 46
Efstathiou, G., Bernstein, G., Tyson, J. A., Katz, N., & Guhathakurta, P. 1991, ApJ, 380, L47
Giovi, F., Baccigalupi, C., & Perrotta, F. 2005, Phys. Rev. D, 71, 103009
Hirata, C. M., Padmanabhan, N., Seljak, U., Schlegel, D., & Brinkmann, J. 2004, Phys. Rev. D, 70, 103501
Hu, W., Scott, D., & Silk, J. 1994, Phys. Rev. D, 49, 648
Jeong, D., & Komatsu, E. 2006, ApJ, 651, 619
Knox, L. 1995, Phys. Rev. D, 52, 4307
Kosowsky, A. 2003, NewA Rev., 47, 939
Nolta, M. R., et al. 2004, ApJ, 608, 10
Peiris, H. V., & Spergel, D. N. 2000, ApJ, 540, 605
Rees, M., & Sciama, D. 1968, Nature, 217, 511
Ruhl, J., et al. 2004, Proc. SPIE, 5498, 11
Sachs, R., & Wolfe, A. 1967, ApJ, 147, 73
Schneider, P. 2005, preprint (astro-ph/0509252)
Seljak, U. 1996, ApJ, 460, 549
Smith, R. E., et al. 2003, MNRAS, 341, 1311
Spergel, D. N., et al. 2007, ApJS, 170, 377
Springel, V. 2005, MNRAS, 364, 1105
Takada, M., & Sugiyama, N. 2002, ApJ, 569, 8
Tegmark, M., & Efstathiou, G. 1996, MNRAS, 281, 1297
Tuluie, R., Laguna, P., & Anninos, P. 1996, ApJ, 463, 15
Verde, L., & Spergel, D. 2002, Phys. Rev. D, 65, 043007